

51. D. Power, personal communication.
52. D. W. Rains and R. C. Valentine, *Genetic Engineering of Osmoregulation* (Plenum, New York, 1980).
53. G. W. Smedes and L. E. Hurd, *Ecology* **62**, 1561 (1981).
54. S. Graham, D. Kirchman, R. Mitchell, *Biol. Bull. (Woods Hole, Mass.)* **159**, 160 (1980).
55. R. Neumann, *Marine Ecology, Prog. Ser.* **1**, 21 (1979).
56. W. E. G. Muller, R. K. Zahn, B. Kurelec, C. Lucu, I. Muller, G. Uhlenbruch, *J. Bacteriol.* **145**, 548 (1981).
57. R. Weiner, in preparation.
58. M. G. Hadfield, *Settlement and Metamorphosis of Marine Invertebrate Larvae* (Elsevier, New York, 1978), p. 165.
59. D. J. Crisp, in *Chemoreception in Marine Organisms*, P. T. Grant and A. M. Mackie, Eds. (Academic Press, New York, 1974), p. 177.
60. D. B. Spangenberg, *J. Exp. Zool.* **178**, 183 (1971).
61. F. P. Veitch and H. Hidu, *Chesapeake Sci.* **12**, 173 (1971).
62. D. P. Morse, H. Duncan, N. Hooker, A. Belour, G. Young, *Fed. Proc. Fed. Am. Soc. Exp. Biol.* **39**, 3237 (1980).
63. D. Kirchman, S. Graham, D. Reish, R. Mitchell, *J. Exp. Mar. Biol. Ecol.* **56**, 153 (1982).
64. V. L. Scofield, J. M. Schlumpbergere, L. A. West, I. L. Weissman, *Nature (London)* **295**, 499 (1982).
65. V. L. Scofield and I. L. Weissman, *Dev. Comp. Immunol.* **5**, 23 (1981).
66. A. Bourdillon, *C. R. Acad. Sci. Paris* **239**, 1434 (1954).
67. W. A. Müller, *Wilhelm Roux's Arch. Dev. Biol.* **173**, 107 (1973).
68. S. Coon, personal communication (1983).
69. R. Weiner and R. R. Colwell, in preparation.
70. R. Mitchell and L. Young, *Tech. Rep. No. 3*, U.S. Office Naval Research Contract No. N00014-67-A-0298-0026 NR-306-025 (1972).
71. D. B. Bonar and M. G. Hadfield, *J. Exp. Mar. Biol. Ecol.* **16**, 227 (1974).
72. R. A. Cameron and R. T. Hinegardner, *Biol. Bull. (Woods Hole, Mass.)* **146**, 335 (1974).
73. The author wishes to thank S. W. Joseph and R. M. Weiner for reading of the manuscript and also Michael Fincham, Jack Greer, and Sandy Harpe for their assistance.

RESEARCH ARTICLE

Mineralogical Information from a New Airborne Thermal Infrared Multispectral Scanner

Anne B. Kahle and Alexander F. H. Goetz

In the past decade, research in geologic remote sensing (1) has focused mainly on the development of techniques to exploit data obtained in the visible and near-infrared region of the spectrum extending from wavelengths between 0.4 and 2.5 μm (2). This region contains spectral features associated with electronic transitions in the transition metals

and diagnostic spectral emission features for silicates. In silicate rocks there is a broad minimum in emissivity between 8 and 11 μm , the reststrahlen band, which results from interatomic stretching vibrations of silicon and oxygen bound in the crystal lattice (5); the depth and position of the band is related to the crystal structure of the constituent

Abstract. A new six-channel aircraft multispectral scanner has been developed to exploit mineral signature information at wavelengths between 8 and 12 micrometers. Preliminary results show that igneous rock units can be identified from their free silica content, and that carbonate as well as clay-bearing units are readily separable on the digitally processed images.

minerals and overtone vibrations in minerals containing hydroxyl and carbonate ions (3). Airborne and spaceborne multispectral scanners obtain images in this region by measuring reflected solar radiation, and the spectral information has been used extensively in geologic mapping (2, 4).

Now, a new airborne instrument, the thermal infrared multispectral scanner (TIMS), has been developed. With this instrument it is possible to obtain spectral emittance data in the thermal infrared, that portion of the electromagnetic spectrum which is dominated by thermal radiation from the earth's surface. In particular, the 8- to 13- μm region con-

minerals. The band center has been shown (5) to move to longer wavelengths and decrease in intensity with decreasing quartz content and the concomitant increase in mafic mineral content. Sheet silicates (clays) also have an aluminum-oxygen-hydrogen bond bending mode feature in addition to the silicon-oxygen stretching features. Carbonate emittance spectra are essentially featureless in this wavelength region.

Early attempts to use multispectral image data in the thermal infrared (6) met with limited success because only two channels of data were available and the radiometric sensitivity of the instrument was inadequate. A sensitive instrument

is required because the contrast in spectral emittance among rocks is usually less than 0.15, while the visible and reflective infrared regions exhibit contrasts of 0.5 or greater. Kahle and Rowan (7) were successful in obtaining data in six thermal infrared channels with an aircraft scanner over the East Tintic Mountains, Utah. While results were promising, the scanner was dismantled shortly thereafter and the experiment could not be repeated.

The TIMS is a six-channel scanner with high radiometric sensitivity that consists of a 19-cm diameter Newtonian reflector telescope mounted behind an object-plane 45° flat scanning mirror and followed by a Czerny-Turner spectrometer (8). In the focal plane, the entrance slit to the spectrometer acts as the field stop and defines the instantaneous field of view of 2.5 mrad. The total field of view scanned is 80°. A six-element mercury-cadmium-telluride detector array, cooled by liquid nitrogen, is mounted at the exit of the spectrometer. The nominal spectral bands covered are 8.2–8.6, 8.6–9.0, 9.0–9.4, 9.4–10.2, 10.2–11.2, and 11.2–12.2 μm . The sensitivity ranges between 0.1° and 0.3°C noise-equivalent temperature change at 300 K. This sensitivity is comparable to a noise-equivalent change in spectral emissivity of 0.002 to 0.006.

Some of the first flights with the TIMS have been over sites previously studied with other remote sensing instruments: Death Valley, California, and the Cuprite mining district in Nevada (Fig. 1). The image data are highly correlated from one spectral channel to the next, mainly because the radiance measured has a strong dependence on surface temperature. The diagnostic information in the multispectral data, however, lies in the emissivity variations as a function of

The authors are, respectively, the supervisor and senior research scientist, of the geology group, Jet Propulsion Laboratory, California Institute of Technology, Pasadena 91109.

wavelength. For this reason, an image-processing technique, based on a principal component transformation, called a decorrelation stretch, is used (9). This technique causes the spectral differences between surface units to be displayed as color differences, while most of the temperature variation is displayed as intensity differences. The colors tend to have the same hue as those in a conventional color composite of the same bands, only they are more saturated. This technique was used successfully with the six-channel multispectral data in the East Tintic Mountains (7).

For the Death Valley site, a color composite of three of the six channels of TIMS data (channels 1, 3, and 5, displayed as blue, green, and red, respectively) was processed with the decorrelation stretch, and a generalized lithologic map of the same area, after Hunt and Mabey (10), was redrawn to illustrate specific features recognizable with the TIMS data (Fig. 2). Death Valley and its surrounding mountains are in the southwestern part of the Great Basin. The eastern edge of the Panamint Mountains is in the left half of the TIMS image (Fig. 2) with alluvial fans spreading eastward down to the floor of Death Valley, seen in the right edge of this image. The westward extension of the Amargosa thrust complex, which lies along the eastern foot of the Panamint Mountains in the southern part of the image, is composed of many kinds of igneous, metamorphic, and sedimentary rocks. The Cambrian and Ordovician rocks displayed in the image are predominantly dolomite, with some shale and limestone, but also include the Eureka Quartzite. The Tertiary volcanic rocks in this area consist mainly of rhyolitic tuffs. Vegetation is sparse or absent.

In our previous work in the East Tintic Mountains (7) we noted that the decorrelation stretch display technique caused silica-rich rocks to be red to red-orange, clay-rich rocks to be a bluish red to purple, and carbonates to be green—colors expected on the basis of laboratory spectral emittance studies of these materials (11). These same general relations appear to be valid in the TIMS image of the Death Valley area. Both the Eureka Quartzite and the Sterling Quartzite stand out in bright red (low emissivity in bands 1 and 3 and high in band 5). The remaining metasediments, which are predominantly spectrally flat carbonates, are blue-green because their emissivity is higher in channels 1 and 3 than other units in the image. The Tertiary volcanics, fan gravels, and valley



Fig. 1. Location map of test sites.

evaporite deposits are all clearly separable by hue. The volcanic rocks, with their emissivity minimum shifted to longer wavelengths than the quartzites, have a magenta appearance (high emissivity in channels 1 and 5 and low in 3).

Details in the hues of the fan gravels appear to be related to source materials for the gravel, erosional age of the surface, and the development of desert varnish on the surface.

The second area for which we have TIMS data, the Cuprite mining district in Nevada, contains both hydrothermally altered and unaltered rocks well exposed at the surface. A visible and near infrared (VNIR) color ratio composite of the area taken from a previous aircraft scanner flight (12) can be compared with the TIMS data for the same area (Fig. 3). The site includes two areas of intense hydrothermal alteration, on either side of Highway 95, which cuts through the center of the images (Fig. 4). Units exposed in the district include Tertiary ash-flow and air-fall tuffs (Thirsty Canyon Formation, Siebert Tuffs), basalt, Cambrian siltstone and orthoquartzite of the upper part of the Harkless Formation, and Cambrian limestone of the Mule Spring Formation. The two alteration zones are more or less centered on the occurrences

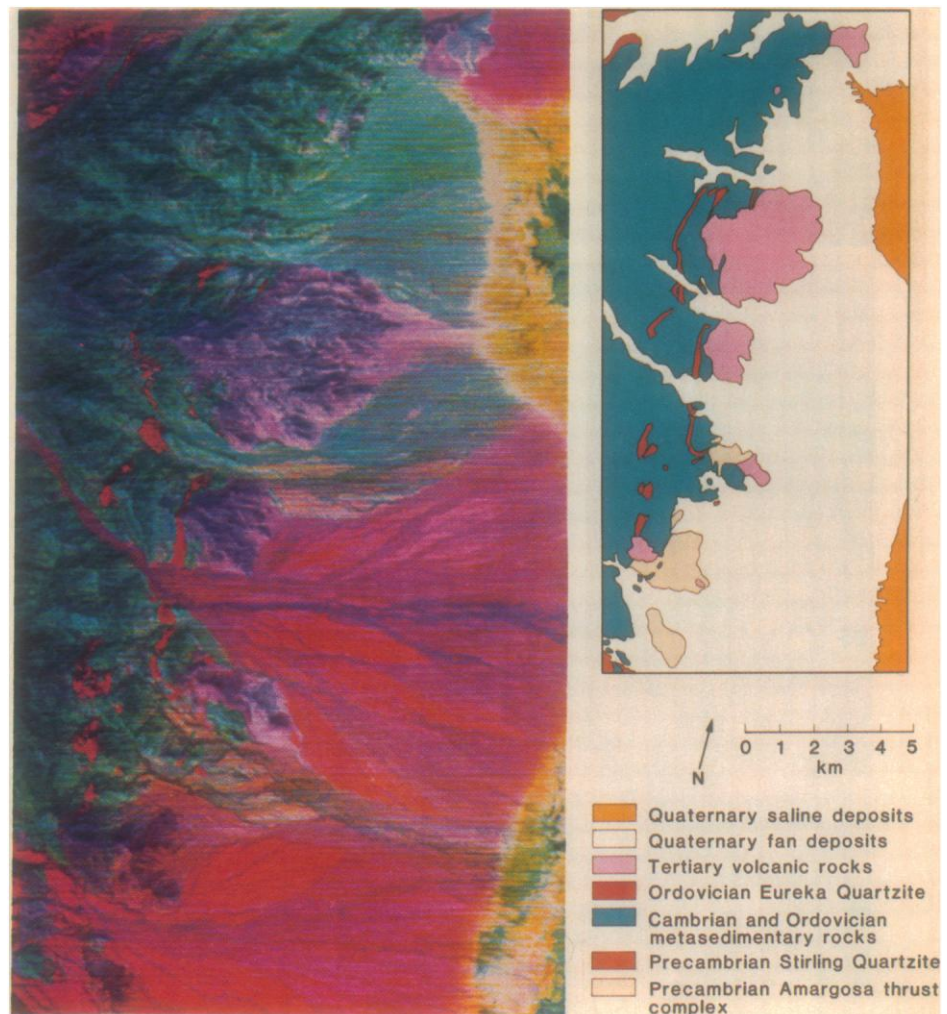


Fig. 2. (Left) A TIMS image of part of the east side of the Panamint Mountains and the west side of Death Valley. (Right) Generalized lithologic map of the same area (10).

of the Siebert unit. The altered rocks have been classified as silicified, opalized, or argillized (13). Vegetation is sparse.

The spectral band ratios used to construct the VNIR color ratio composite are 1.6/2.2 displayed in red, 1.6/0.48 in green, and 0.6/1.0 in blue (12). These were chosen to best delineate the altered

rocks in the image. The hydroxyl-bearing minerals in the altered rocks have a large ratio (1.6/2.2) and hence appear reddish. Iron-rich rocks have a high ratio (1.6/0.48) and have a green component in the image. The silicified rocks, with most of the clays removed, appear dark red to brown and locally bluish purple to blue. The clay-rich opalized rocks vary from

magenta to red to yellow. The argillized rocks are yellow to green (clay plus iron). Unaltered rocks are predominantly dark green, dark blue, and black.

The TIMS image of Cuprite was processed in the same manner as the Death Valley image. Because the statistics used for the transformations of the images are unique for each image and dependent on the relative abundance of spectral types within the image, the relations between colors and mineralogy will vary somewhat from one area to another but are recognizable. The TIMS image clearly delineates the altered rocks. The silicified rocks (S) are bright orange, and the clay-rich opalized units (O) are magenta. These colors correspond directly to the mapped (13) occurrence of the alteration.

Both VNIR and TIMS images of the Cuprite district delineate the altered zones, but for different reasons. In the VNIR image, distinctions are based primarily on clay and alunite content of the rocks and, in this area, on a very minor limonite content. In the TIMS image the discrimination is based primarily on the free-silica content and to some extent on the clay content. This difference can be noted specifically in the silicified core of the altered zone where the alteration is most intense. In the VNIR image this unit appears dark, as do the unaltered units, because most of the clays have been removed leaving only hydrothermal quartz. In the TIMS image it is clearly a distinctive orange unit, indicative of the high quartz content.

In addition, it is possible on the TIMS image to distinguish among several of the unaltered rock types. Here the basalt (B) and unaltered tuffs (T) are blue-green, the carbonates (C) bright green, and the unaltered Harkless siltstone (SS) light yellow-green. These distinctions cannot be made from the VNIR image, where all these units are spectrally similar and appear dark blue to black.

It is interesting to compare the alluvial fans on the VNIR and TIMS images. Both delineate the fans and intrafan units in a variety of colors, but there is not a one-to-one relation between the areas delineated. In the VNIR image, for instance, there is a small blue fan (Q) just south of the eastern altered zone that contrasts with the surrounding pink fans. It appears to be the same blue as the fans at the eastern edge of the image. On the TIMS image, however, this fan is pink and similar in color to its surroundings but dissimilar from the easternmost fans, which appear yellow. In general, it can be said that the colors of fans on the



Fig. 3. (Top) A VNIR color ratio composite of the Cuprite mining district and (bottom) a TIMS image of the same area. Abbreviations: B, basalt; C, carbonates; O, opalized units; Q, small blue fan; S, silicified rocks, SS, Harkless siltstone; and T, unaltered tuffs.

TIMS image are related to the composition of the source material or the development of desert varnish on the surface, or both. The alluvial material in the VNIR images often appears dissimilar from its source material, and the spectral reflectance is determined primarily by the development of weathering products on the surface.

The TIMS is a powerful new geologic remote-sensing tool that can provide mineralogical information, particularly about silicate rocks, that is not available from sensors in other wavelength regions. After modification and calibration, TIMS will become part of the complement of NASA aircraft research instruments.

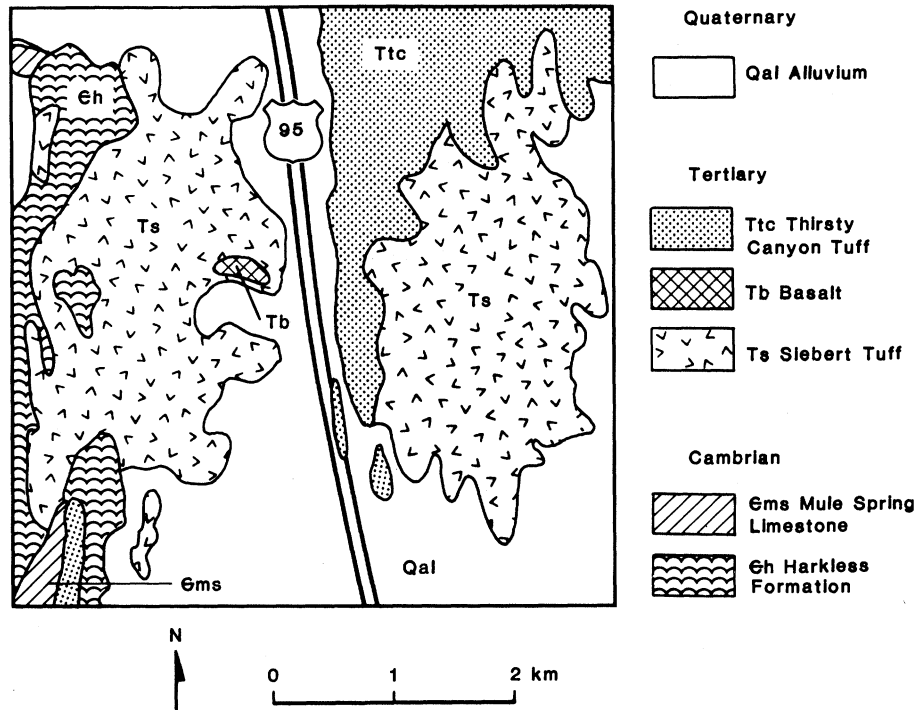


Fig. 4. Generalized lithologic map of the Cuprite mining district (12), redrawn from Albers and Stewart (14).

References and Notes

1. Remote sensing is defined here as the acquisition of information about a surface based on the analysis of emitted or reflected electromagnetic radiation in the wavelength region 0.4 μm to 50 cm.
2. L. C. Rowan, P. H. Wetlaufer, A. F. H. Goetz, F. C. Billingsley, J. H. Stewart, *U.S. Geol. Surv. Prof. Pap.* 883 (1974); A. F. H. Goetz and L. C. Rowan, *Science* 211, 781 (1981); B. S. Siegal and A. R. Gillespie, Eds., *Remote Sensing in Geology* (Wiley, New York, 1980).
3. G. R. Hunt, *Geophysics* 42, 501 (1977).
4. G. L. Raines, T. W. Offield, E. S. Santos, *Econ. Geol.* 73, 1706 (1978); R. Viljoen, M. Viljoen, J. Grootenboer, T. Longshaw, *Miner. Sci. Eng.* 7, 132 (1975); M. Podwysocki, F. Gunther, A. Blodgett, *Goddard Space Flight Center Doc.* 923-77-17 (1977); R. Houston, *Univ. Wyo. Contrib. Geol.* 12, 77 (1974); G. Bailey and P. Anderson, *Bull. Am. Assoc. Pet. Geol.* 66, 1348 (1982).
5. P. J. Launer, *Am. Mineral.* 37, 764 (1952); R. J. P. Lyon, *Econ. Geol.* 60, 715 (1965); G. R. Hunt and J. W. Salisbury, *U.S. Air Force Cambridge Res. Lab. Rep.* AFCRL-TR-74-0625 (1974); *ibid.* AFCRL-TR-75-0356 (1975); *ibid.* AFCRL-TR-76-0003 (1976).
6. R. K. Vincent and F. Thomson, *J. Geophys. Res.* 77, 2465 (1972); _____, K. Watson, *ibid.* p. 2473.
7. A. B. Kahle and L. C. Rowan, *Geology* 8, 234 (1980).
8. To collect the images shown here, the TIMS was flown in a Gates Lear Jet by NASA's National Space Technology Laboratory (NSTL) at an altitude of 40,000 feet.
9. A. B. Kahle, D. P. Madura, J. M. Soha, *App. Opt.* 19, 2279 (1980).
10. C. B. Hunt and D. R. Mabey, *U.S. Geol. Surv. Prof. Pap.* 494-A (1966).
11. G. Hunt, personal communication.
12. M. J. Abrams, R. P. Ashley, L. C. Rowan, A. F. H. Goetz, A. B. Kahle, *Geology* 5, 736 (1977).
13. R. P. Ashley and M. J. Abrams, *U.S. Geol. Surv. Open File Rep.* 80-367 (1980).
14. J. P. Albers and J. H. Stewart, *Nev. Bur. Mines Geol. Bull.* 78 (1972).
15. We appreciate the support of NASA/NSTL, in particular G. Flanagan in the construction and flight-testing of TIMS, and thank M. J. Abrams and A. R. Gillespie of the Jet Propulsion Laboratory for their constructive suggestions. This research was carried out under contract to NASA. Daedalus Enterprises constructed the TIMS under contract to NASA.

8 April 1983; revised 24 June 1983